Transactions Letters

High-Throughput High-Performance TDMA Through Pseudo-Orthogonal Carrier Interferometry Pulse Shaping

Balasubramaniam Natarajan, *Member, IEEE*, Carl R. Nassar, *Senior Member, IEEE*, and Steve Shattil

***Abstract*—This letter provides a novel method for doubling throughput in time division multiple access (TDMA) systems. Specifically, with pseudo-orthogonal positioning of carrier interferometry pulse shapes, a TDMA system is designed to support twice as many real symbols in a slot, without increasing bandwidth or slot duration. With regard to performance, the doubling of throughput comes at the cost of only 1–2 dB performance degradations at probability of error of 10^{-2}.**

***Index Terms*—Frequency domain equalization, multicarrier modulation, pulse shaping, time division multiple access (TDMA).**

I. Introduction

TIME DIVISION multiple access (TDMA) systems such as the Global System for Mobile Communications (GSM) are extremely popular in wireless communication environments worldwide. In [1] and [2], a new implementation of TDMA, named carrier interferometry/TDMA (CI/TDMA), is introduced. At the transmitter, each information symbol modulates a novel pulse shape (the CI pulse shape) created by the superposition of N carriers equally spaced in frequency. In CI/TDMA receivers, equalizers are replaced by: 1) fast-Fourier transforms (FFTs) which decompose each pulse shape into its carrier components and 2) a frequency combiner creating frequency diversity benefits. The CI/TDMA system demonstrates 5–8 dB gains at bit-error-probability of 10^{-2} over a TDMA system employing Gaussian pulse shaping and a decision feedback equalizer [DFE(6,4)]. These performance benefits result because the proposed frequency domain processing overcomes the performance degradations experienced by digital matched filters and equalizers with a limited number of taps [e.g., ten taps in the case of DFE(6,4)].

In this letter, we demonstrate that we can tradeoff some of the performance gains achieved in the CI/TDMA system for increases in throughput. Specifically, we extend the concept of pseudo-orthogonality, used with success in CDMA systems, to increase capacity in CI/TDMA. (For examples of the success of pseudo-orthogonal codes to increase CDMA capacity, see, e.g., [3]–[5], where the result of this code design is refered to as "oversaturation" or "channel overloading"). In [6], the idea of pseudo-orthogonal codes was first extended to TDMA, where pseudo-orthogonal information bearing signals were deployed. Here, gains in throughput (far less than 100%) were provided at a cost of considerable increases to receiver complexity.

In this work, we propose the extension of the pseudo-orthogonality concept to CI/TDMA where it provides a 100% gain in capacity with no cost in receiver complexity, bandwidth, or slot duration, and only a small cost in performance. Specifically, by positioning the CI pulse shapes pseudo-orthogonally at the transmitter, the number of real transmitted symbols per slot is doubled. This intentional introduction of intersymbol interference (ISI) at the transmitter introduces performance degradations at the receiver. With enough new pulse shapes in a burst to double throughput, the performance of CI/TDMA introduced in [1] and [2] is degraded by only 1–2 dB at a bit-error-probability of 10^{-2}.

II. Pseudo-Orthogonal Pulse Shaping

The CI pulse shape employed in the CI/TDMA transmitter is created by superpositioning N carriers equally spaced in frequency by $\Delta f = 1/T_s$, where N corresponds to the number of symbols per slot, e.g., 148 in GSM, and T_s is the TDMA slot time. The CI pulse corresponds to

$$h(t) = \sum_{i=0}^{N-1} A e^{j(i2\pi\Delta f t)} \tag{1}$$

where $A = \sqrt{1/N}\sqrt{1/T_s}$ is a constant that ensures a pulse energy of unity (over T_s).

The pulse shape $h(t)$ of (1) may be implemented at low cost by application of a lookup table (assuming the pulse has been computed in advance). Alternatively, in the case of a software defined radio system implementing, e.g., multicarrier code-division multiple-access (MC-CDMA) or orthogonal frequency-division multiplexing (OFDM), the pulse shape $h(t)$ can instead be implemented by using the existing inverse fast Fourier transform (required for OFDM/MC-CDMA transmission). This makes CI/TDMA well suited for co-existence with, e.g., OFDM systems, in future software defined radios.

Manuscript received December 23, 2001; revised August 15, 2002, January 20, 2003, and February 4, 2003; accepted February 26, 2003. The editor coordinating the review of this paper and approving it for publication is M. Sawahashi. This work was supported by 2000 Colorado Advanced Software Institute Grant, "Carrier Interference Pulse Shaping for improved TDMA Capacity and Performance (CIMA)."

B. Natarajan is with the Department of Electrical and Computer Engineering, Kansas State University, Manhattan, KS 66502 USA (e-mail: bala@ksu.edu).

C. R. Nassar is with the Department of Electrical and Computer Engineering, Colorado State University, Ft. Collins, CO 80523-1373 USA (e-mail: carln@engr.colostate.edu).

S. Shattil is with the Idris Communications, Superior, CO 80027 USA (e-mail: steve@idriscomm.com).

Digital Object Identifier 10.1109/TWC.2004.826318

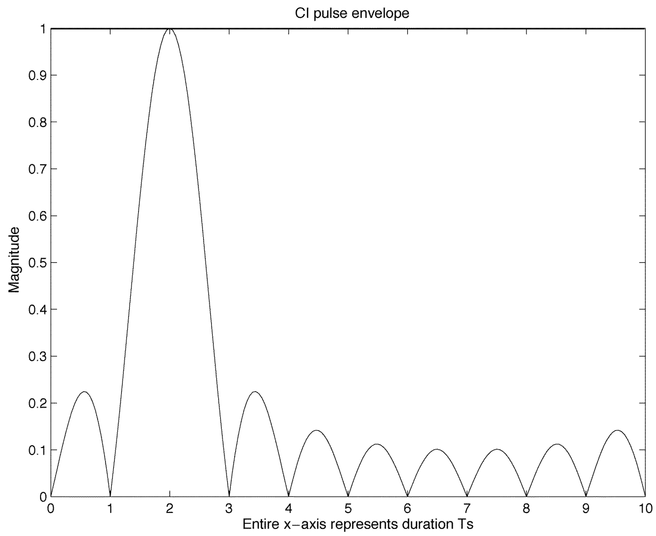

Fig. 1. CI pulse shape ($N = 10$).

Fig. 1 plots the envelope of the pulse shape $h(t)$ over the slot time T_s (with a delay of "2" introduced for ease in presentation). As seen in Fig. 1, the CI pulse shape extends over the entire slot duration T_s (576.6 μs in GSM) and not bit duration T_b (3.69 μs in GSM).

To transmit a TDMA burst of symbols, the kth symbol in a user's burst a_k is modulated by the CI pulse shape $h(t - \tau_k)$, creating the total transmitted signal

$$s(t) = \Re e \left\{ \sum_{k=0}^{K-1} a_k h(t - \tau_k) e^{j2\pi f_c t} \right\} \cdot g(t). \tag{2}$$

Here, a_k is assumed to be $+1$ or -1 supporting both ease in presentation and assuring real signaling (i.e., BPSK is assumed), $g(t)$ refers to the rectangular function that extends over a slot duration (T_s), f_c is the carrier frequency, and K is the total number of symbols in a slot. It is important to note that the time-shifted pulses $h(t - \tau_k)$ and $h(t - \tau_j)$ are orthogonal over slot duration T_s if and only if $\tau_k = kT_b$ and $\tau_j = jT_b$, i.e.,

$$\int_0^{T_s} h(t - kT_b) h^*(t - jT_b) dt = 0 \quad (k \neq j; k, j \in I) \tag{3}$$

where * represents the complex conjugate.

From (3), it is evident that the CI/TDMA system supports N orthogonal pulse shapes positioned at $\{kT_b, k = 0, 1, \ldots, N - 1\}$. However, it is possible to support additional pulse shapes in a time slot by positioning the CI pulses pseudo-orthogonally, i.e., selecting τ_k and τ_j such that $\int_0^{T_s} h(t - \tau_k) h(t - \tau_j) dt \leq \epsilon$, where ϵ is some small predetermined value.

In this letter, we allow the first N pulse shapes to be placed orthogonally, i.e., located at positions $\{\tau_k = kT_b, k = 0, 1, \ldots, N - 1\}$. Now, if we introduce a fixed delay ζ, i.e., replace each τ_k by $\tau_k - \zeta$, the set of pulse shapes remain orthogonal to one another. That is, the cross correlation between the pulse shapes remains zero as long as the difference is $\tau_m - \tau_n = (mT_b - \zeta) - (nT_b - \zeta) = (m - n)T_b$. Of course, there is correlation between an orthogonal set of N pulse shapes with $\zeta = 0$ and the orthogonal set of N pulse shapes constructed with arbitrary ζ.

We seek to support $2N$ pulse shapes in one TDMA slot duration, by simultaneously supporting one set of N pulse shapes with $\zeta = 0$ and another orthogonal set with $\zeta = \zeta$. To do this in an optimal fashion, we determine the value of ζ that minimizes the root mean square (rms) cross correlation between the set $h(t), h(t - T_b), \ldots, h(t - (N - 1)T_b)$ and the set $h(t - \zeta), h(t - T_b - \zeta), \ldots, h(t - (N - 1)T_b - \zeta)$ in the case of real signaling. Mathematical analysis (see Appendix A) yields an intutively pleasing result, namely that when positioning the $2N$ pulse shapes in a slot, each pulse shape should be separated from the neighboring pulse shapes by duration $T_b/2$ (i.e., $\zeta = T_b/2$). This is most easily understood in terms of the transmitter output

$$s(t) = \Re e \left\{ \sum_{k=0}^{2N-1} a_k h\left(t - k\frac{T_b}{2}\right) e^{j2\pi f_c t} \right\} \cdot g(t) \tag{4}$$

$$s(t) = \Re e \left\{ \sum_{k=0}^{2N-1} a_k \sum_{i=0}^{N-1} A e^{j\left(2\pi f_c t + 2\pi i \Delta f\left(t - k\frac{T_b}{2}\right)\right)} \right\} \cdot g(t). \tag{5}$$

Notice that $2N$ symbols have been positioned in the same slot duration T_s by separating pulses by duration $T_b/2$ rather than the usual T_b.

III. Bandwidth Efficiency

A TDMA system using Nyquist root raised cosine pulse shaping with a rolloff factor α has a total radio-frequency (RF) bandwidth $BW_{rc} = ((1 + \alpha)/T_b) = (1 + \alpha)R_b$ (where R_b is the data rate, i.e., $R_b = (1/T_b)$). If a Gaussian pulse shape is employed with $BT = 0.3$ (typical of GSM systems), 99% of the power is contained in bandwidth $BW_g = 1.8R_b$ [7].

In CI/TDMA, the transmitted signal is the sum of time-limited sinusoids (see (2), and recall that $h(t)$ is a sum of sinusoids and $g(t)$ is a rectangular waveform of duration T_s). In the frequency domain, each time-limited sinusoid maps to a sinc function with 1) a total power of $1/N$th the transmit power (since the transmit power is spread evenly over all N carriers) and 2) a null-to-null bandwidth occupancy of $2/T_s$. Considering 1) the spectral overlap among the orthogonal carriers (as in OFDM and MC-CDMA [8], [9]) and 2) the fact that the sidelobes of each sinc waveform are of extremely low power (since each sinc waveform containes $1/N$th of the transmit energy, e.g., 1/148 of the transmit energy), it is reasonable to assume (and commonplace in the multicarrier literature to assume) that the spectral occupancy of a CI/TDMA transmit signal is very well approximated by

$$BW_{CI} = N\Delta f = N \cdot \frac{1}{NT_b} = \frac{1}{T_b} = R_b. \tag{6}$$

Thus, we see that CI/TDMA systems demonstrate the bandwidth efficiency of a sinc pulse shape. This is not a surprising result as the CI pulse shape can be perceived as a frequency sampled version of the standard sinc pulse.

Specifically, the CI/TDMA system has a spectral occupancy that is 80% less than that of GMSK $(BT = 0.3)$, when both are

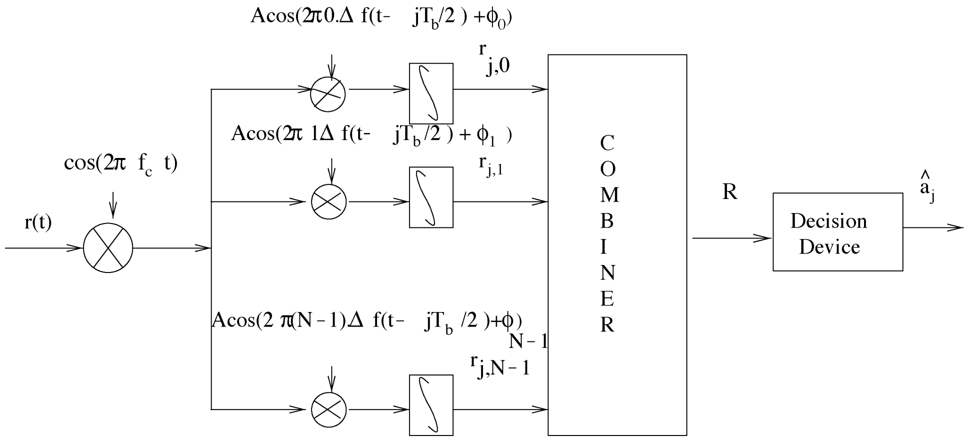

Fig. 2. CI/TDMA receiver structure.

designed to support identical data rates. When compared to systems employing raised cosine pulse shapes with $\alpha = 1$ (with the same data rate), the CI/TDMA system occupies only one half of $BW_{\rm rc}$. Furthermore, when we consider the pseudo-orthogonal pulse shapes of Section II for doubling the data rate (without increasing $BW_{\rm CI}$), the bandwidth efficiency gains (measured in b/s/Hz) in CI/TDMA are in the order of 260%, 300%, and 100% relative to GMSK (with $BT = 0.3$), a raised cosine pulse (with $\alpha = 1$) and a sinc pulse, respectively.

IV. Receiver Structure

A multipath fading channel is assumed. In traditional TDMA systems, multipath components create intersymbol interference (ISI) and time-based processing, namely equalizer or MLSE receiver structures, are deployed to combat this interference in the time domain. However, considering the transmit signal of (5), it is evident that this signal is a multicarrier signal, and, as such, receivers can be constructed in the frequency domain, in a manner consistent with traditional OFDM [8] or MC-CDMA [10] reception. Since we want to support frequency domain receivers, the multipath effect in the time domain is mapped to a frequency selectivity in the frequency domain. (This is consistent with existing literature on multicarrier transmissions, e.g., OFDM [8] and MC-CDMA [10]). Here, while frequency selectivity exists over the entire TDMA transmit bandwidth, it is reasonable to assume that each of the individual carriers making up the transmit signal experience a unique flat fade (a direct consequence of a large N value). In other words, typical of a multicarrier system, the carriers resolve the frequency selectivity, leading to the received signal of the form

$$r(t) = \sum_{k=0}^{2N-1} a_k \sum_{i=0}^{N-1} \alpha_i A \cdot \cos\left(2\pi f_c t + 2\pi i \Delta f\left(t - k\frac{T_b}{2}\right) + \phi_i\right) g(t) + \eta_i(t) \quad (7)$$

where α_i is the gain, ϕ_i the phase offset in the i^{th} carrier of the CI pulse shape (due to the channel fade), and $\eta_i(t)$ is additive white Gaussian noise (AWGN). There is a correlation between subcarrier fades α_i and α_j where the degree of correlation is provided in [11]. These fades are generated using the algorithm in [12]. It is the uniqueness of the fade and phase offset per carrier that makes the channel a multipath channel (frequency selective). That is, as a result of unique values of fade gain and phase offset (per carrier), the orthogonality between pulse shapes is destroyed. [It is also important to note that the authors assume a guard time between TDMA bursts, typical of TDMA systems such as GSM. These guard times are normally of sufficient length to ensure no ISI between bursts (i.e., the guard time in CI/TDMA acts much the same way as a cyclic prefix in OFDM. To perfectly emulate the effect of a cyclic prefix, a short signal transmission may be permitted in the guard interval). The presence of such a guard time is implicitly assumed when presenting (7).]

Fig. 2 illustrates the CI/TDMA receiver's detection of the jth symbol. Here, the jth symbol residing on the CI pulse shape, $h(t - jT_b/2)$, is separated into its N component frequencies (implementable via an FFT). This results in a decision vector $\underline{\mathbf{r}}_j = (r_{j,1}, r_{j,2}, \ldots, r_{j,N})$ where $r_{j,i}$ is the ith carrier component and corresponds to

$$r_{j,i} = A\alpha_i a_j + \sum_{l=0, l\neq j}^{2N-1} A\alpha_i a_l \cos\left(2\pi i \Delta f\left(j\frac{T_b}{2} - l\frac{T_b}{2}\right)\right) + \eta_{j,i}. \quad (8)$$

Here, the second term represents ISI and the third term $\eta_{j,i}$ is a Gaussian random variable with mean 0 and variance $N_0/2$. Next, the receiver implements a combining across the N vector components using minimum mean square error combining (MMSEC) to minimize ISI and optimize frequency diversity benefits. The MMSEC has been shown to be both 1) far superior to other commonly used combining strategies (e.g., orthogonality restoration combining, equal gain combining) [9] and 2) a very close approximation to the truly optimal maximum likelihood (ML) combining strategy [13]. Employing MMSEC leads to the decision statistic (see Appendix B)

$$R_j = \sum_{i=1}^{N} r_{j,i} \cdot \left[\frac{\alpha_i}{\left(\alpha_i^2 \sum_{p=1}^{2N} \cos\left(2\pi i \Delta f\left(p\frac{T_b}{2} - j\frac{T_b}{2}\right)\right)^2 + \frac{N_o}{2}\right)}\right]. \quad (9)$$

A hard decision device provides the final output $\hat{a}_j$.

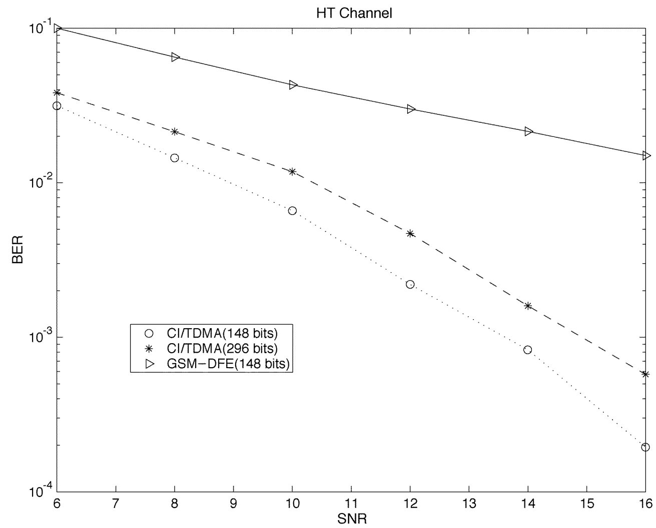

Fig. 3. BER comparison in HT channel.

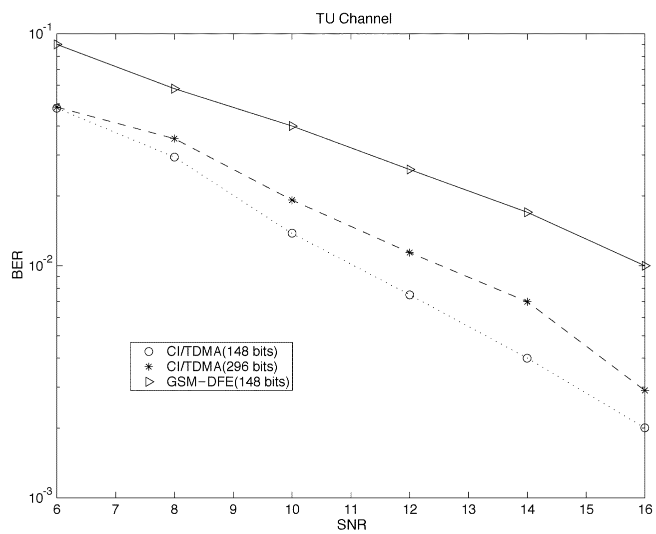

Fig. 4. BER comparison in TU channel.

V. Performance Results

Figs. 3 and 4 present bit-error probability (BER) versus SNR performance curves for a BPSK TDMA system operating over the hilly terrain (HT) (rms delay spread of 5.03 μs) and typical urban (TU) (rms delay spread of 1.06 μs) channels [15], respectively. We assume the channel is slowly fading and is constant over one frame interval (i.e., Doppler spread is negligible [14]). We also assume perfect knowledge of the channel fade parameters and ideal noise power estimate (available via appropriate training/tracking schemes) and the performance results we present do not include channel coding gains.

The solid line represents a benchmark GSM system with $N = 148$ symbols per burst employing Gaussian pulse shaping with a DFE(6,4) receiver [16]. Our reasons for selecting the particular benchmark for comparison are two-fold: 1) the DFE equalizer structure has been shown to demonstrate performances very close to that of the optimal MLSE with its Viterbi decoder [16] and 2) the complexity of a DFE receiver is (approximately speaking) very close to that of the proposed frequency-based receiver employing MMSEC.

The dotted line marked with circles represents the performance of the CI/TDMA system with $N = 148$ orthogonal pulses shown in [1] and [2]. This CI/TDMA system was designed to support the GSM bit rate of 270.8 kb/s and occupies a bandwidth of $BW_{CI} = 270.8$ kHz (see Section III). The dashed line marked with stars demonstrates the performance of the CI/TDMA system with double throughput (296 symbols per burst) via pseudo-orthogonal positioning (bandwidth occupancy remains 270.8 kHz and slot duration is unchanged). Relative to the CI/TDMA system with $N = 148$ symbols per burst, the novel CI/TDMA architecture demonstrates degradations of 1–2 dB, resulting from the ISI introduced at the transmitter side. This performance degradation is small when compared to the doubling in throughput. Moreover, with 296 b/slot, the CI/TDMA system achieves close to 6.5 dB gain relative to GSM with Gaussian pulse shaping and a DFE(6,4) receiver at BER of 10^{-2} in a HT channel. In the TU channel, gains in the order of 4 dB are achieved at probability of errors in the order of 10^{-2}. These results were obtained with no increase in bandwidth (BW_{CI}) or burst duration.

VI. Conclusion

In this letter, we proposed a CI/TDMA system employing real signaling supporting twice the throughput of traditional TDMA systems without increasing burst duration or bandwidth, by positioning CI pulse shapes pseudo-orthogonally in time at positions $k(T_b/2)$. Using a receiver that employs suitable combining techniques the system loses only 1–2 dB relative to CI/TDMA with orthogonal pulse positioning (and half the throughput). In summary, by application of the pseudo-orthogonality concept that has found widespread use in CDMA, TDMA systems with real signaling can now benefit from significant gains in throughput. Future work involves the extension of this concept to higher-order/complex constellations such as QPSK and QAM.

Appendix A
Minimizing RMS Correlation

Let $R_{1,2}(m,n)$ refer to the cross correlation between the mth pulse shape in orthogonal set 1 (constructed with $\zeta = 0$) and the nth pulse shape in orthogonal set 2 (constructed with $\zeta = \zeta$). Also let

$$R_{\mathrm{rms}} = \left[\frac{1}{N^2}\sum_{m=0}^{N-1}\sum_{n=0}^{N-1} R_{1,2}^2(m,n)\right]^{\frac{1}{2}} \tag{10}$$

represent the rms cross correlation that exists between pulse shapes in set 1 and set 2 (a measure of the amount of inter-symbol-interference). We seek to find the value for ζ that minimizes R_{rms}. Now, it is easily shown that

$$R_{1,2}(m,n) = \sum_{i=0}^{N-1} e^{j(2\pi i \Delta f(mT_b - nT_b - \zeta))} \tag{11}$$

Furthermore, assuming real signaling, e.g., BPSK transmission, only the real part of the cross correlation determines the amount of interference and, hence

$$R_{1,2}(m,n)=\sum_{i=0}^{N-1}\cos\left(2\pi i\Delta f(mT_b-nT_b-\zeta)\right). \quad (12)$$

It is also easy to show that

$$\sum_{m=0}^{N-1}R_{1,2}^2(m,n)=\sum_{m=0}^{N-1}R_{1,2}^2(m,n') \quad n\neq n'. \quad (13)$$

That is, the total cross correlation between the nth pulse shape in orthogonal set 2 and all the pulse shapes in set 1 is identical to the cross-correlation between the (n')th pulse shape in orthogonal set 2 and all the pulse shapes in set 1. Using (13), we can rewrite (10) as

$$R_{\text{rms}}=\left[\frac{1}{N}\sum_{m=0}^{N-1}R_{1,2}^2(m,0)\right]^{\frac{1}{2}} \quad (14)$$

and using (12), this becomes

$$R_{\text{rms}}=\left[\frac{1}{N}\sum_{m=0}^{N-1}\left(\sum_{i=0}^{N-1}\cos\left(2\pi i\Delta f(mT_b-\zeta)\right)\right)^2\right]^{\frac{1}{2}}. \quad (15)$$

We now determine the selection of ζ for set 2 that minimizes the rms correlation, R_{rms}, between the two sets of pulse shapes. To do this, we select

$$\frac{\partial R_{\text{rms}}}{\partial\zeta}=0 \quad (16)$$

$$\frac{\partial R_{\text{rms}}}{\partial\zeta}=\frac{1}{2}\left[\frac{1}{N}\sum_{m=0}^{N-1}R_{1,2}^2(m,0)\right]^{-\frac{1}{2}}\frac{1}{N}\cdot I \quad (17)$$

where

$$\begin{aligned}I&=\frac{\partial\left[\sum_{m=0}^{N-1}R_{1,2}^2(m,0)\right]}{\partial\zeta}\\&=\frac{\partial\left[\sum_{m=0}^{N-1}\left(\sum_{i=0}^{N-1}\cos\left(2\pi i\Delta f(mT_b-\zeta)\right)\right)^2\right]}{\partial\zeta}. \quad (18)\end{aligned}$$

Now

$$\begin{aligned}I&=\sum_{m=0}^{N-1}2\left[\sum_{i=0}^{N-1}\cos\left(2\pi i\Delta f(mT_b-\zeta)\right)\right]\\&\quad\cdot\left[\sum_{k=0}^{N-1}k\sin\left(2\pi k\Delta f(mT_b-\zeta)\right)\right]\\&=\sum_{m=0}^{N-1}\sum_{i=0}^{N-1}\sum_{k=0}^{N-1}2k\cos\left(2\pi i\Delta f(mT_b-\zeta)\right)\\&\quad\times\sin\left(2\pi k\Delta f(mT_b-\zeta)\right)\\&=\sum_{m=0}^{N-1}\sum_{i=0}^{N-1}\sum_{k=0}^{N-1}k\left[\sin\left(2\pi(k+i)\Delta f(mT_b-\zeta)\right)\right.\\&\quad\left.+\sin 2\pi(k-i)\Delta f(mT_b-\zeta)\right]\\&=\Im m\left[\sum_{m=0}^{N-1}\sum_{i=0}^{N-1}\sum_{k=0}^{N-1}k\left(e^{j(2\pi(k+i)\Delta f(mT_b-\zeta))}\right.\right.\\&\quad\left.\left.+e^{j(2\pi(k-i)\Delta f(mT_b-\zeta))}\right)\right]\\&=\Im m\left[\sum_{i=0}^{N-1}\sum_{k=0}^{N-1}ke^{-j(2\pi(k+i)\Delta f\zeta)}\right.\\&\quad\left.\times\sum_{m=0}^{N-1}e^{j(2\pi(k+i)\Delta fmT_b}\right]\\&\quad+\Im m\left[\sum_{i=0}^{N-1}\sum_{k=0}^{N-1}ke^{-j(2\pi(k-i)\Delta f\zeta)}\right.\\&\quad\left.\times\sum_{m=0}^{N-1}e^{j(2\pi(k-i)\Delta fmT_b}\right]\\&=\Im m\left[\sum_{i=0}^{N-1}\sum_{k=0}^{N-1}ke^{-j(2\pi(k+i)\Delta f\zeta)}\delta(k+i-N)N\right]\\&\quad+\Im m\left[\sum_{i=0}^{N-1}\sum_{k=0}^{N-1}ke^{-j(2\pi(k-i)\Delta f\zeta)}\delta(k-i)N\right]\\&=\Im m\left[\sum_{i=0}^{N-1}(N-i)e^{-j(2\pi N\Delta f\zeta)}+\sum_{i=0}^{N-1}i\right]\cdot N. \quad (19)\end{aligned}$$

When $\zeta=(k/2N\Delta f)$, $k=0,1,\ldots$, we have $I=0$ and, therefore, from (17), $(\partial R_{\text{rms}}/\partial\zeta)=0$.

Seeking to determine which ζ are maxima and which are minima, we calculate the second order partial derivative at $\zeta=(k/2N\Delta f)$ and determine

$$\begin{aligned}\frac{\partial R_{\text{rms}}^2}{\partial^2\zeta}&>0 \quad \text{when} \quad \zeta=\frac{(2k+1)}{2N\Delta f}\\\frac{\partial R_{\text{rms}}^2}{\partial^2\zeta}&<0 \quad \text{when} \quad \zeta=\frac{2k}{2N\Delta f}. \quad (20)\end{aligned}$$

Hence, $\zeta=(2k/2N\Delta f)$ corresponds to a maxima and $\zeta=((2k+1)/2N\Delta f)$ provides minima. Selecting $k=0$, we choose $\zeta=(1/2N\Delta f)$ as our minima. Using $(1/N\Delta f)=T_b$ leads to the final result

$$\zeta=\frac{T_b}{2}. \quad (21)$$

APPENDIX B
CALCULATING MINIMUM MEAN SQUARED ERROR COMBINING WEIGHTS

The minimum mean square error combining method approximates the transmitted symbol a_k from the N-length vector, $\underline{\mathbf{r}}_j$, by the linear sum

$$R_j=\sum_{i=1}^{N}r_{j,i}\cdot w_i. \quad (22)$$

Based on the MMSE criterion, the weights w_i are selected to ensure that the estimation error is orthogonal to all the baseband components of the received subcarriers [17]. That is

$$E\left\{\left(a_k - \sum_{i=1}^{N} w_i r_{j,i}\right) \cdot r_{j,i}\right\} = 0, \quad i = 1, 2, \ldots, N. \quad (23)$$

The solution to (23) as obtained from Weiner filter theory corresponds to [18]

$$w_i = C^{-1} A \quad (24)$$

where $C = E\{r_{j,i} \cdot r_{j,i} | \alpha_i\}$, $A = E\{a_k \cdot r_{j,i} | \alpha_i\}$ and $E\{\cdot\}$ denotes the expected value. The operation of (24), when applied to the $r_{j,i}$ in CI/TDMA with BPSK modulation, yields

$$C = \alpha_i^2 \sum_{p=1}^{2N} \cos\left(2\pi i \Delta f \left(p\frac{T_b}{2} - j\frac{T_b}{2}\right)\right)^2 + \frac{N_o}{2} \quad (25)$$

$$A = \alpha_i. \quad (26)$$

Substituting (25) and (26) in (24), we obtain the weights for MMSEC

$$w_i = \frac{\alpha_i}{\left(\alpha_i^2 \sum_{p=1}^{2N} \cos\left(2\pi i \Delta f \left(p\frac{T_b}{2} - j\frac{T_b}{2}\right)^2 + \frac{N_o}{2}\right)}. \quad (27)$$

References

[1] B. Natarajan, C. R. Nassar, and S. Shattil, "Innovative pulse shaping for high-performance wireless TDMA," *IEEE Commun. Lett.*, vol. 5, pp. 372–374, Sept. 2001.

[2] ——, "Exploiting frequency diversity in TDMA through carrier interferometry," in *Proc. Wireless 2000, 12th Int. Conf. Wireless Communications*, vol. 2, Calgary, AB, Canada, July 10–12, 2000, pp. 469–476.

[3] R. E. Learned, A. S. Willisky, and D. M. Boroson, "Low complexity joint detection for oversaturated multiple access communications," *IEEE Trans. Signal Processing*, vol. 45, pp. 113–122, Jan 1997.

[4] F. Vanhaverbeke, M. Moeneclaey, and H. Sari, "DS/CDMA with two sets of orthogonal spreading sequences and iterative detection," *IEEE Commun. Lett.*, vol. 4, pp. 289–291, Sept. 2000.

[5] J. A. F. Ross and D. P. Taylor, "Vector assignment scheme for M+N users in N-dimensional global additive channel," *Electron. Lett.*, vol. 28, Aug. 1992.

[6] F. Vanhaverbeke, M. Moeneclaey, and H. Sari, "An excess signaling concept with Walsh-Hadamard spreading and joint detection," in *Proc. Globecom 2000 Conf. Rec.*, vol. 2, San Fransisco, CA, Nov. 2000, pp. 906–909.

[7] T. S. Rappaport, *Wireless Communications—Principles and Practice*, 1st ed. Englewood Cliffs, NJ: Prentice-Hall, 1996.

[8] R. Prasad, *OFDM for Wireless Multimedia Communications*. Norwood, MA: Artech House, Jan. 2000.

[9] S. Hara and R. Prasad, "Overview of multi-carrier CDMA," *IEEE Commun. Mag.*, vol. 35, pp. 126–133, Dec. 1997.

[10] N. Yee, J. P. Linnartz, and G. Fettweia, "Multi-carrier CDMA in indoor wirelss radio," in *Proc. IEEE Int. Conf. Personal, Indoor, and Mobile Radio Communications*, Dec. 1993, pp. 109–113.

[11] W. C. Jakes, Ed., *Microwave Mobile Communications*. New York: IEEE Press, 1974.

[12] B. Natarajan, C. R. Nassar, and V. Chandrasekhar, "Generation of correlated Rayleigh fading envelopes for spread spectrum applications," *IEEE Commun. Lett.*, vol. 4, pp. 9–11, Jan. 2000.

[13] Z. Wu, C. R. Nassar, and S. Lu, "Maximum likelihood combining for MC-CDMA," in *Proc. IEEE Vehicular Technology Conf.*, vol. 3, VTC Spring, 2002, pp. 1293–1297.

[14] J. G. Proakis, *Digital Communications*. New York: McGraw-Hill, 1995.

[15] "Digital land mobile radio communications," Commission of the European Community, Brussels, Belgium, Final rep. of the COST-Project 207, 1989.

[16] B. A. Bjerke, J. G. Proakis, M. K. Lee, and Z. Zvonar, "A comparison of decision feedback equalization and data directed estimation technique for the GSM system," in *Proc. IEEE 6th Int. Conf. Universal Personal Communications*, vol. 1, 1997, pp. 84–88.

[17] Z. Leon-Garcia, *Probability and Random Processes for Electrical Engineering*, 2nd ed. Reading, MA: Addison-Wesley, 1994.

[18] S. Haykin, *Adaptive Filter Theory*. Englewood Cliffs, NJ: Prentice-Hall, 1991.